Thermally induced escape: The principle of minimum available noise energy

R. L. Kautz
National Bureau of Standards, Boulder, Colorado 80303
(Received 1 March 1988)

The average time required for thermally induced escape from a basin of attraction increases exponentially with inverse temperature in proportion to $\exp(E_A/kT)$ in the limit of low temperature. A minimum principle states that the activation energy E_A is the minimum available noise energy required to execute a state-space trajectory which takes the system from the attractor of the noise-free system to the boundary of its basin of attraction and that the minimizing trajectory is the most probable low-temperature escape path. This principle is applied to the problem of thermally induced escape from two attractors of the dc-biased Josephson junction, the zero-voltage state and the voltage state, to determine activation energies and most probable escape paths. These two escape problems exemplify the classical case of escape from a potential well and the more general case of escape from an attractor of a nonequilibrium system. Monte Carlo simulations are used to verify the accuracy of the activation energies and most probable escape paths derived from the minimum principle.

I. INTRODUCTION

Deterministic nonlinear dynamical systems often possess more than one steady-state solution for a given set of parameters. The relative stability of such solutions is a question of practical importance in a variety of systems including electronic circuits, lasers, and particle accelerators where a particular steady state is desired.[1] In some cases it is sufficient to know the local stability of a solution as determined by the system's response to infinitesimal perturbations. However, information regarding global stability is usually more relevant to real-world systems where disturbances are necessarily finite. Measures of local stability such as Lyapunov exponents are relatively easy to calculate because they depend only on the equation of motion linearized about the steady-state solution. Although measures of global stability, which depend on the full nonlinear response of the system, are usually more difficult to evaluate, the information obtained often provides a qualitatively different picture than local stability measures. An extreme example of this difference results for chaotic steady-state solutions which are globally stable but locally unstable.[2]

For dissipative systems a natural measure of global stability can often be derived from the response of the system to thermal noise. The presence of dissipation in a system has two important consequences. First, dissipation implies the existence of noise at nonzero temperatures as described by the fluctuation-dissipation theorem. Second, dissipation implies that each steady-state solution of the noise-free system is represented by an attractor and a surrounding basin of attraction in state space. If initial conditions are chosen within a given basin of attraction then the eventual steady-state behavior of the noise-free system is motion on the associated attractor. At small but nonzero temperatures, thermal noise produces motion in which the system occasionally jumps from one basin of attraction to another but is almost always found close to an attractor. Under these conditions, the mean time τ required for escape from a basin of attraction is a useful measure of the attractor's global stability.

The classical problem of thermally induced escape from a potential well is a special case of escape from a basin of attraction. For the potential-well problem, the temperature dependence of the mean escape time is dominated in the limit of low temperature by the Arrhenius factor $\exp(E_A/kT)$, where E_A, the activation energy, is the barrier height of the potential well.[3] Because the escape time depends exponentially on the activation energy, E_A is usually the most important parameter defining the stability of a potential minimum. A problem of current interest is the extension of escape calculations to nonequilibrium systems in which the dynamics cannot be reduced to the motion of a particle in a potential well and/or the attractor is a trajectory rather than a fixed point.[4] A general solution to the problem of thermally induced escape from a basin of attraction has been formulated[5–7] in terms of a quasipotential defined over state space. In this formulation the mean escape time exhibits an Arrhenius factor with an activation energy which is the minimum difference in quasipotential between the boundary of the basin of attraction and the attractor. Thus, the use of E_A as a measure of global stability can be extended to a range of complex systems that cannot be modeled by a particle in a potential well.

The quasipotential, which characterizes the response of a system to weak thermal noise, satisfies a Hamilton-Jacobi equation defined over state space. An analogy can be drawn between this Hamilton-Jacobi equation and that of classical mechanics, which establishes a minimum principle for thermal noise problems equivalent to the principle of least action.[5,8–10] According to this principle, the difference in quasipotential between a given point in a basin of attraction and the associated attractor

is related to the most probable trajectory by which the system can move from the attractor to the given point under the influence of weak thermal noise. The most probable path is that which minimizes an actionlike quantity and the difference in quasipotential is the minimum of this action. In thermal-noise problems, the actionlike quantity associated with a trajectory is the available noise energy required to execute the trajectory.[11] Stated in physical terms, the difference in quasipotential between a given point and the attractor is thus the minimum available noise energy required to move from the attractor to the given point. Application of this minimum principle allows differences in quasipotential to be evaluated by solving an ordinary differential equation rather than a Hamilton-Jacobi partial differential equation.

Because the activation energy for thermally induced escape is the minimum difference in quasipotential between the basin boundary and the attractor, it is also the minimum available noise energy required to execute movement from the attractor to the basin boundary. In previous work,[11] a calculational method based on the principle of minimum available noise energy was used to evaluate the activation energy for escape from both a periodic attractor and a chaotic attractor. The method was demonstrated to be simple, efficient, and applicable to complex problems. The principle of minimum available noise energy thus provides a practical way of evaluating the global stability of steady-state solutions for a wide range of nonlinear nonequilibrium systems.

Here we develop this calculational technique in greater detail by applying it to a simple system, the dc-biased Josephson junction. The dynamical behavior of the dc-biased junction is equivalent to that of a particle in a tilted sinusoidal potential in the presence of linear damping. The system is a useful test case because it includes coexisting fixed-point and periodic attractors. Escape from the fixed-point attractor corresponds to escape from a potential well and provides a good test of the minimum principle because the activation energy is known exactly. The potential-well case is also of interest because the most probable low-temperature escape trajectory is known to be the time reversal of the path by which the system relaxes from the basin boundary to the attractor.[11] Here we verify this identity by comparing the reverse relaxation trajectory both with the escape trajectory that minimizes the required available noise energy and with low-temperature escape paths computed by Monte Carlo methods. Escape from the periodic attractor represents a more general case for which exact analytic solutions for the low-temperature limit are not known. The accuracy of calculations based on the minimum principle is demonstrated for this case by comparison with Monte Carlo simulations and available analytic approximations. The Monte Carlo simulations also confirm that the most probable escape path is that requiring the minimum available noise energy. However, the reverse relaxation trajectory is distinctly different from the most probable escape path in this case, revealing that results for potential wells do not always apply to the general problem of escape from an attractor.

II. NOISE-FREE SYSTEM

The system to be considered consists of an ideal Josephson element with critical current I_c shunted by a capacitance C and resistance R and driven by a dc bias I_0 as shown in Fig. 1. The Johnson noise of the resistance is represented by the noise current I_N. In normalized units, the equation of motion for the difference in superconducting phase ϕ across the junction is[12,13]

$$\beta\ddot{\phi}+\dot{\phi}+\sin\phi=i_0+i_N(t) , \tag{1}$$

where $\beta=2eI_cR^2C/\hbar$ is a dimensionless parameter which varies inversely with damping, $i_0=I_0/I_c$ is the normalized dc bias, $i_N=I_N/I_c$ is the normalized noise current, t is the time measured in units of $\hbar/2eI_cR$, and dots indicate derivatives with respect to t. The noise current associated with the Johnson noise of the resistance is represented by a white Gaussian process with an impulsive autocorrelation function,[14]

$$\langle i_N(t)i_N(t')\rangle=2\Gamma\delta(t-t') , \tag{2}$$

where $\Gamma=2ekT/\hbar I_c$ is the temperature normalized to the Josephson coupling energy. In this notation, $\dot{\phi}$ is the junction voltage measured in units of I_cR.

In the absence of noise ($\Gamma=0$), Eq. (1) is a deterministic dissipative system having steady-state solutions which correspond to attractors in state space. Before taking up the subject of noise-induced transitions between attractors, we focus on the state-space structure of the attractors and basin boundaries in the noise-free system.

Physical insight into the nature of the attractors can be gained by recognizing that the dynamical behavior of the noise-free system is equivalent to the autonomous motion of a particle in a potential subject to linear damping. That is, the equation of motion takes the form

$$\beta\ddot{\phi}+\dot{\phi}+U'(\phi)=0 , \tag{3}$$

where U' is the derivative with respect to ϕ of the potential

$$U(\phi)=-i_0\phi-\cos\phi . \tag{4}$$

This potential, often called the washboard potential, consists of a sinusoidal component plus a linear ramp with a slope determined by the dc bias i_0. For $|i_0|<1$, the potential has local minima at the points

$$\phi_{\min}=\sin^{-1}i_0+2n\pi , \tag{5}$$

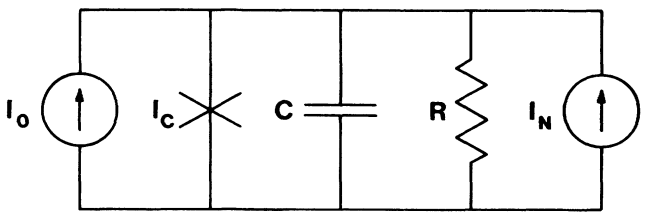

FIG. 1. Circuit diagram for the dc-biased Josephson junction.

and local maxima at the points

$$\phi_{\max} = -\sin^{-1} i_0 + (2n+1)\pi \ , \tag{6}$$

where n is an integer. For $|i_0| > 1$ the potential is a monotonic function of ϕ and there are no local minima.

The washboard potential is plotted in Fig. 2(a) for $i_0 = 0.2$. Inspection of this figure suggests that two types of steady-state solution are possible for $|i_0| < 1$. One consists simply of the particle at rest at a potential minimum and corresponds to a fixed-point attractor in state space. The other, permitted when the slope is sufficiently steep for a given damping, consists of steady

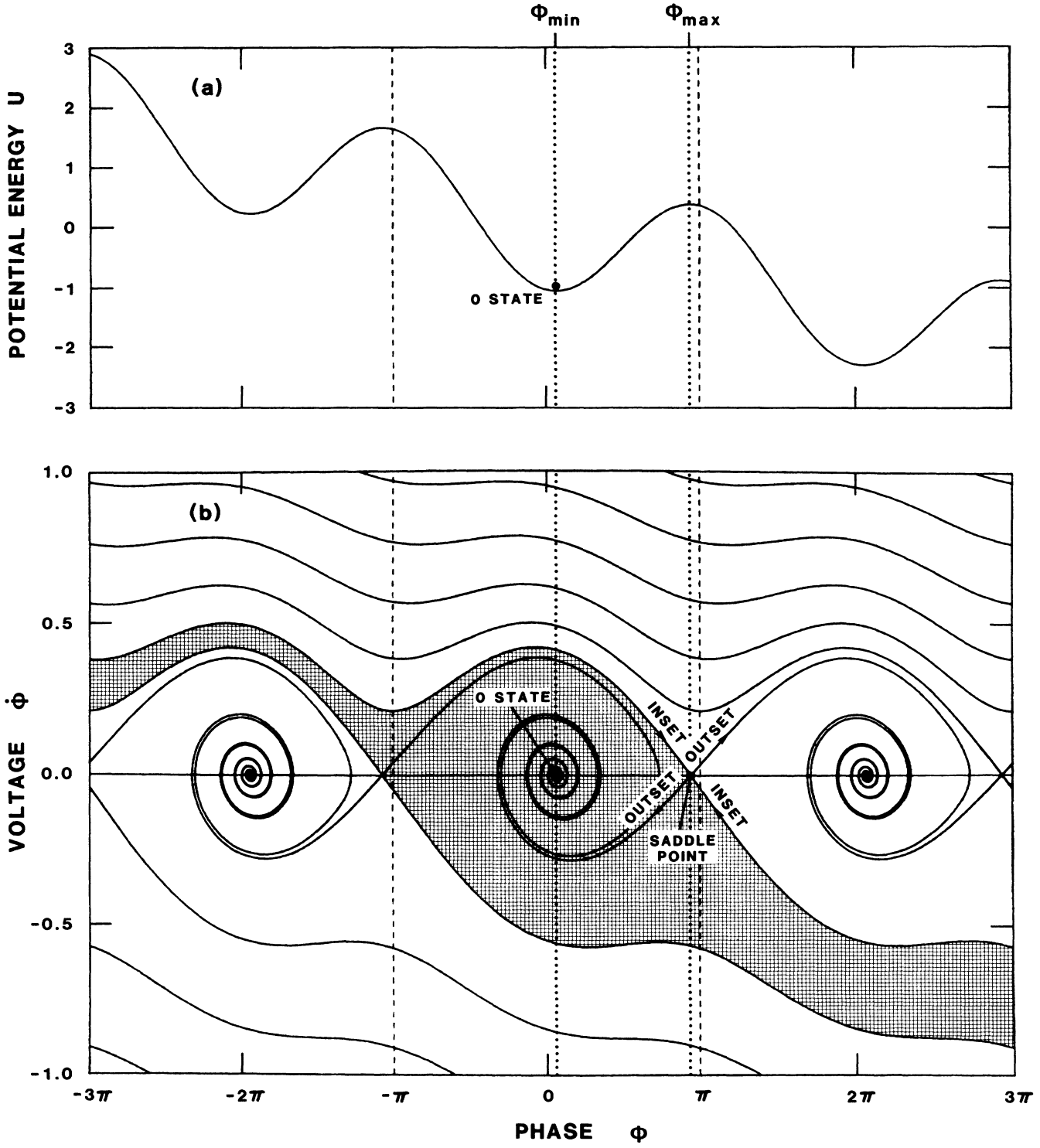

FIG. 2. Potential energy (a) and state-space portrait (b) of the noise-free system for $i_0 = 0.2$ and $\beta = 25$. The basin of attraction for the fixed point nearest $\phi = 0$ is indicated by crosshatching. Potential energy is in units of $\hbar I_c / 2e$ and voltage is in units of $I_c R$.

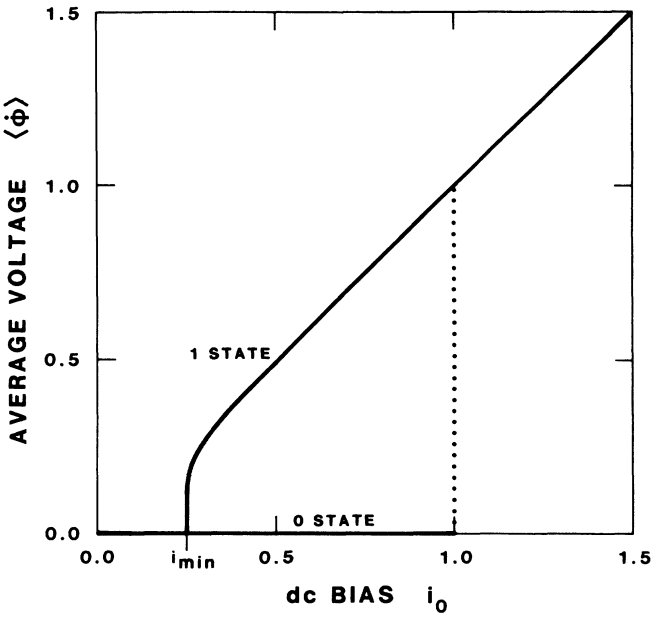

FIG. 3. Time average of the voltage (units of I_cR) as a function of normalized dc bias for steady-state solutions of Eq. (3). The hysteresis parameter is $\beta=25$.

motion down the potential ramp with a velocity modulated by the undulations of the potential. This running solution can be described as a periodic attractor if we assume that ϕ is taken modulo 2π as appropriate to a Josephson junction. The stationary and running solutions of a junction are called the zero-voltage state and the voltage state but here are called simply the 0 state and the 1 state. These two states and noise-induced transitions between them are the primary focus of the present work.

The dc-bias ranges of the 0 state and 1 state are shown in the current-voltage characteristic plotted in Fig. 3 for a case, $\beta=25$, corresponding to relatively light damping. The 0 state exists for $|i_0|<1$ where the potential possesses local minima. The 1 state exists for $|i_0|>i_{\min}$ where the slope of the potential is sufficient to offset damping losses and steady-state motion can be maintained. The parameter $i_{\min}$ is 0.2521 in the present case but can vary between 0 and 1 depending on β.[12,13]

For $|i_0|<1$ there are an infinite number of coexisting attractors for the washboard potential, namely the fixed points associated with the potential minima at $\phi_{\min}$. For $|i_0|<i_{\min}$ these fixed points are the only attractors of the system. Figure 2(b) is a state-space portrait illustrating this situation for $i_0=0.2$ and $\beta=25$. In this diagram, the attractors are located at the points $(\phi,\dot{\phi})=(\phi_{\min},0)$. The basin of attraction for the attractor at $(\sin^{-1}i_0,0)$ is indicated by crosshatching. For any set of initial conditions $(\phi(0),\dot{\phi}(0))$ chosen within this area, the final state of the system will be the 0 state at $\phi=\sin^{-1}i_0$. The boundaries of the basins of attraction are determined by the set of unstable fixed points associated with the maxima of the potential. These fixed points, located at $(\phi_{\max},0)$, are called saddle points because they are stable with respect to perturbations in some state-space directions and unstable with respect to perturbations in other directions. Each saddle point has associated with it a stable and an unstable manifold or inset and outset. By definition, motion beginning at a point on the inset asymptotically approaches the saddle point. Each inset defines a boundary between two basins of attraction. The outset is the collection of trajectories along which the system relaxes from the saddle point to an attractor. There are two outset trajectories in the present case, connecting the saddle point with the two adjacent attractors. The outset trajectories are of interest because they define the possibilities for the most probable escape trajectory in potential-well problems.

For $i_{\min}<|i_0|<1$ the system has a periodic attractor in addition to the fixed-point attractors and the state-space topology takes the form shown in Fig. 4(b). In this figure ϕ is plotted modulo 2π and all of the fixed-point attractors are considered to be equivalent to the 0 state at $\phi=\sin^{-1}i_0$. The periodic attractor is the wavy trajectory extending from $-\pi$ to π that is repeatedly traversed when the system is in the 1 state. The boundary separating the basins of the 0 state and 1 state is again the inset of the saddle point at $\phi=\pi-\sin^{-1}i_0$. The basin of the 0 state is indicated by crosshatching and its complement is that of the 1 state.

The state-space portraits shown in Figs. 2(b) and 4(b) define the escape problems to be considered in the following sections. In the presence of thermal noise a system initialized on a given attractor is forced by the random fluctuations of i_N to leave the attractor and wander about in the neighboring state space. Escape occurs when this random motion takes the system across the boundary of the basin of attraction. In later sections we search for the most probable trajectory by which noise can move the system between the attractor and the basin boundary to produce an escape event.

Before leaving the noise-free system, we examine the character of autonomous motion in the neighborhood of the system's three steady states: the stable and unstable fixed points and the periodic attractor. This analysis is necessary to a description of the numerical methods used to calculate inset and outset trajectories and also provides insight into the nature of the most probable escape trajectories discussed in later sections. Given that $\phi_s(t)$ is a steady-state solution, we wish to examine a nearby trajectory of the form

$$\phi(t)=\phi_s(t)+\delta(t)\ , \tag{7}$$

where $\delta(t)$ is assumed to be infinitesimal. Using the fact that both ϕ and ϕ_s are solutions of Eq. (3), we obtain an equation for δ,

$$\beta\ddot{\delta}+\dot{\delta}+(\cos\phi_s)\delta=0\ , \tag{8}$$

which has been linearized as appropriate for an infinitesimal δ. For all three types of steady state, the general solution of Eq. (8) has the form

$$\delta=A_+(t)\exp(S_+t)+A_-(t)\exp(S_-t)\ . \tag{9}$$

Here A_+ and A_- are periodic functions with the same

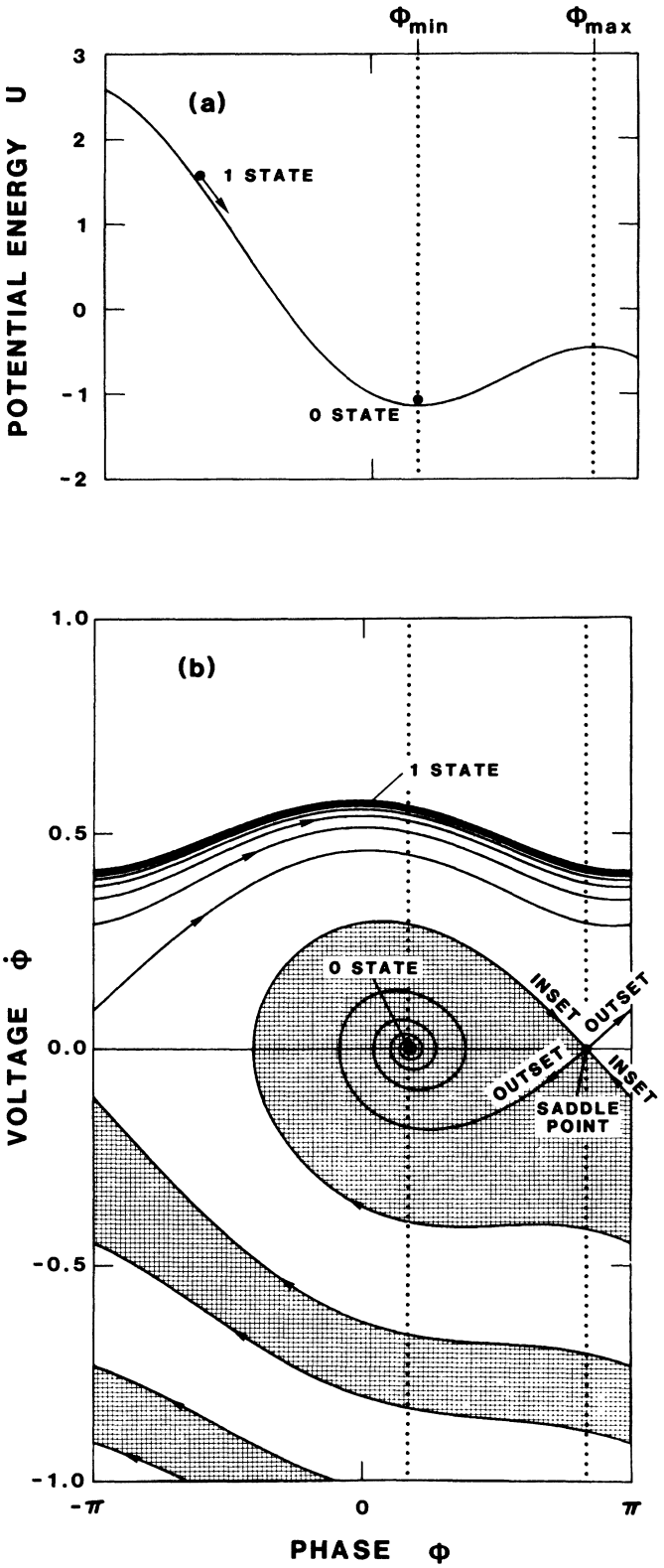

FIG. 4. Potential energy (a) and state-space potrait (b) of the noise-free system for $i_0=0.5$ and $\beta=25$. Here ϕ is plotted modulo 2π and all fixed-point attractors are considered equivalent. The basin of attraction of the 0 state is indicated by crosshatching.

period as ϕ_s in the case of the periodic attractor[15] and constants in the case of the fixed points. The exponents S_+ and S_- are the parameters of greatest interest in Eq. (9) since they determine whether the trajectories near a given steady-state solution converge to the steady state ($\mathrm{Re}[S_\pm]<0$) or diverge from it ($\mathrm{Re}[S_\pm]>0$).

For the given system, the exponents S_+ and S_- satisfy the sum rule[16,17]

$$S_+ + S_- = -\frac{1}{\beta} . \tag{10}$$

In addition, for the periodic solution one of the exponents is identically zero because the system responds neutrally to state-space displacements along the periodic trajectory.[17] These two facts allow us to conclude that for the periodic attractor

$$S_{p\pm} = -\frac{1}{2\beta}(1\pm 1) , \tag{11}$$

such that all trajectories near the periodic attractor converge to it exponentially in a characteristic time β. This behavior is illustrated in Fig. 4(b) by the way in which one of the outset trajectories of the saddle point approaches the 1 state.

For the fixed points there is no requirement that one of the exponents S_+ or S_- be zero because there is no motion associated with the solution. However, since ϕ_s is a constant equal to either $\phi_{\min}$ or $\phi_{\max}$, Eq. (8) is a linear equation with constant coefficients and the exponents are determined by the associated characteristic equation. The results for the stable and unstable fixed points are

$$S_{s\pm} = -\frac{1}{2\beta}\{1\pm[1-4\beta(1-i_0^2)^{1/2}]^{1/2}\} \tag{12}$$

and

$$S_{u\pm} = -\frac{1}{2\beta}\{1\pm[1+4\beta(1-i_0^2)^{1/2}]^{1/2}\} , \tag{13}$$

respectively, assuming $|i_0|<1$. Inspection of Eq. (12) reveals that the real parts of $S_{s\pm}$ are necessarily negative and the the imaginary parts are nonzero if $4\beta(1-i_0^2)^{1/2}>1$. Thus, all solutions in the neighborhood of the stable fixed point approach $(\phi_{\min},0)$ exponentially and if β is sufficiently large the approach exhibits damped oscillations. Such a damped oscillatory approach to the 0 state is again illustrated in Fig. 4(b) by one of the outset trajectories of the saddle point.

For the unstable fixed point, inspection of Eq. (13) reveals that S_{u+} and S_{u-} are both real with $S_{u+}>0$ and $S_{u-}<0$. Thus, trajectories beginning near the saddle point may either converge toward or diverge from $(\phi_{\max},0)$ depending the direction of their initial displacement from this point. The displacement directions yielding the most rapid convergence and divergence coincide with the directions of the inset and outset trajectories, respectively, at the saddle point. A knowledge of these directions forms a starting point for numerical evaluation of the inset and outset. If we define the displacement vector $\Delta(t)=[\delta(t),\dot{\delta}(t)]$ then its time evolution is given by $\Delta(t)=\mathbf{J}(t)\Delta(0)$ where the Jacobian matrix $\mathbf{J}(t)$ can be

written as

$$\mathbf{J}(t)=\begin{bmatrix}\delta_1(t) & \delta_2(t)\\ \dot{\delta}_1(t) & \dot{\delta}_2(t)\end{bmatrix}, \tag{14}$$

where δ_1 and δ_2 are solutions of Eq. (8) satisfying the initial conditions

$$\delta_1(0)=1, \quad \dot{\delta}_1(0)=0 , \tag{15}$$

and

$$\delta_2(0)=0, \quad \dot{\delta}_2(0)=1 . \tag{16}$$

The eigenvalues of $\mathbf{J}$ are $\exp(S_{u\pm}t)$ and the corresponding eigenvectors are

$$\Delta_{\pm}=[1,S_{u\pm}] . \tag{17}$$

The displacement vector Δ_+ defines the direction of most rapid divergence from the saddle point and is tangent to the outset. To compute the outset trajectories, we select a starting point displaced a small distance from $(\phi_{\max},0)$ in the $\pm\Delta_+$ direction and then integrate Eq. (3) to determine how the system relaxes from the saddle point to one of the attractors. Similarly, Δ_- defines the direction of most rapid convergence to the saddle point and is tangent to the inset. To compute the inset trajectories, we select a starting point displaced a small distance from $(\phi_{\max},0)$ in the $\pm\Delta_-$ direction and then integrate Eq. (3) backward in time to determine the origin of trajectories which approach the saddle point. Because the attractors are the asymptotic limits of the outset trajectories and the boundaries between basins of attraction coincide with the inset trajectories, the inset and outset taken together largely define the escape problem to be considered in the following sections.

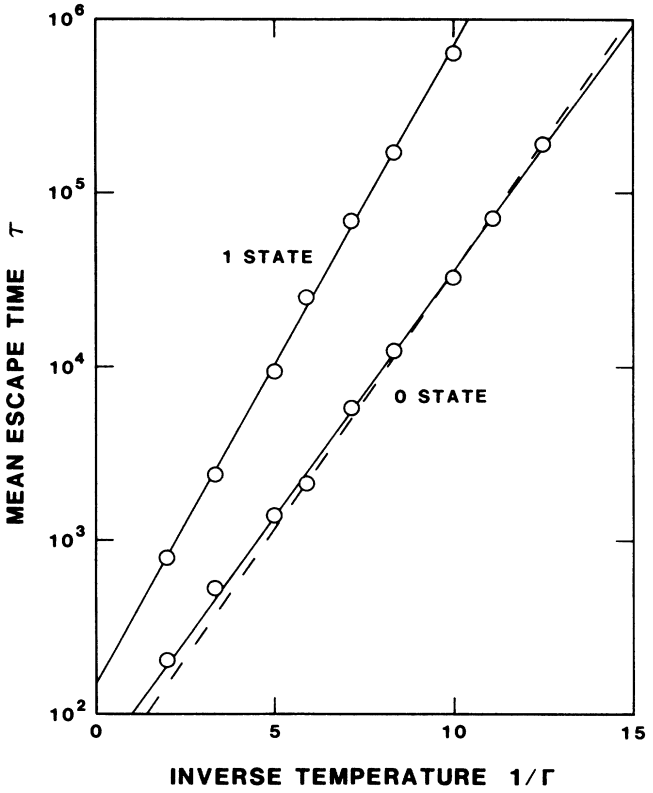

FIG. 5. Mean escape time (units of $\hbar/2eI_cR$) for the 0 state and 1 state as a function of inverse temperature for $i_0=0.5$ and $\beta=25$. Each circle is the average of t_e over 100 Monte Carlo escape events. Solid lines represent least-squares fits to the Monte Carlo points and the dashed line is the analytic result for escape from the 0 state given by Eq. (25).

III. MINIMUM PRINCIPLE

Although there exists rigorous justification for the calculation of activation energies using the principle of minimum available noise energy,[5,8–10] we examine here an informal proof which establishes the principle by a direct argument that provides insight into its physical origins.[11] As a first step, we consider the computation of escape times and activation energies by Monte Carlo simulations.

An escape event can be simulated by numerical integration of the noise-affected equation of motion, Eq. (1) in the present case, with the noise term represented by a random number generator. The mean escape time τ is computed as the average over a series of trials of the time t_e required for the system to move from the attractor of interest to its basin boundary under the influence of noise. For each trial, integration is begun at $t=0$ with the system initialized on the attractor and proceeds by solving for the state of the system at a succession of later times spaced at intervals Δt. The noise source is approximated by assuming that its value is constant over the mth time interval at a value $\bar{i}_N(m)$ that is the average of $i_N(t)$ over the interval

$$\bar{i}_N(m)=\frac{1}{\Delta t}\int_{(m-1)\Delta t}^{m\Delta t} i_N(t)dt . \tag{18}$$

Because $i_N(t)$ is a white Gaussian noise source with an autocorrelation function given by Eq. (2), the random variables $\bar{i}_N(m)$ are uncorrelated and have identical Gaussian distributions with zero mean and variance $2\Gamma/\Delta t$. A Gaussian random number generator can thus be used to represent the noise source in numerical integration of Eq. (1). For each trial, integration is continued until the time t_e when the system first happens to cross the boundary of the basin of attraction. The fact that the random motion of the system is due to white Gaussian noise ensures that escape will occur with probability 1 within a finite time.[7] The mean escape time τ is estimated by the average of t_e over a series of trials with uncorrelated noise waveforms.

Monte Carlo results for the mean escape time of the 0 state and 1 state are plotted in Fig. 5 as a function of inverse temperature for a case in which both states are stable in the absence of noise. The relevant attractors and basins of attraction are those shown in Fig. 4(b). τ is calculated for the 0 state as an average over escape events in which integration is initialized at $(\phi_{\min},0)$ and continued until the system is found to leave the crosshatched

area of Fig. 4(b). Similarly, τ for the 1 state is obtained from Monte Carlo trails in which integration is initialized at a point on the periodic attractor and continued until the system enters the crosshatched area. Each of the circles in Fig. 5 represents the average escape time for 100 such trials.

As Fig. 5 shows, the mean escape times obtained from Monte Carlo simulations for both the 0 state and 1 state increase exponentially with inverse temperature. That is, the temperature dependence of τ approximates that of the Arrhenius factor $\exp(E_A/kT)$ as is expected in the limit of low temperatures. If we introduce a dimensionless activation energy ε_A which is E_A measured in units of the Josephson coupling energy $\hbar I_c/2e$, then the Arrhenius factor takes the form $\exp(\varepsilon_A/\Gamma)$. By fitting a straight line to the data points in Fig. 5 and measuring its slope, we obtain an estimate of ε_A directly from the Monte Carlo simulations. Activation energies obtained in this way provide an important check on results obtained from the principle of minimum available noise energy. Because the activation energy is defined by the low-temperature asymptote, the accuracy of Monte Carlo estimates can be affected if high-temperature points are included in the fitting procedure. For this reason, data points for which the resulting Arrhenius factor was less than 4 were excluded from consideration. To obtain an accurate evaluation of the slope, the included points were also required to span at least 2 orders of magnitude in τ. Using a least-squares fit to the data points shown in Fig. 5, we obtain activation energies of $\varepsilon_A=0.65\pm0.04$ and $\varepsilon_A=0.85\pm0.05$ for the 0 state and 1 state, respectively. The error bounds associated with these numbers represent the values of the slope of the fitting line at which the rms error exceeds its minimum value by a factor of 2.

The inner workings of the Monte Carlo simulation for noise-induced escape can be used to develop the principle of minimum available noise energy as follows. Suppose that the escape rate $1/\tau$ is to be written as the sum of the contributions from all possible escape paths. By an escape path we mean a trajectory that takes the system from the attractor to its basin boundary in some time t_e. The contribution to $1/\tau$ from a particular path is assumed to be proportional to the probability that the path occurs. However, the equation of motion establishes a one-to-one correspondence between escape paths and noise waveforms so the probability of a given escape path is the probability of the noise waveform required to produce it. The numerical technique used in the Monte Carlo simulation suggests a way of computing this probability. If a path is broken into M discrete time intervals of length $\Delta t=t_e/M$ as in numerical simulations, then its probability is the product of the probabilities of the $\bar{i}_N(m)$ values needed to produce it. A product form follows from the fact that the $\bar{i}_N(m)$ are independent random variables. Because all $\bar{i}_N(m)$ have identical Gaussian distributions with variance $2\Gamma/\Delta t$, the escape time can be expressed as

$$1/\tau=\sum_{\text{paths}} F_p \prod_{m=1}^{M} \exp[-\bar{i}_N^2(m)\Delta t/4\Gamma] , \tag{19}$$

where F_p is a path-dependent normalization factor. Converting the product of exponential factors to a sum on exponents and taking the limit as $\Delta t\to 0$ yields

$$1/\tau=\sum_{\text{paths}} F_p \exp(-\varepsilon_N/\Gamma) , \tag{20}$$

where

$$\varepsilon_N=\tfrac{1}{4}\int_0^{t_e} i_N^2 dt . \tag{21}$$

If the temperature dependence of F_p is weaker than exponential, then in the limit of low temperatures the term in Eq. (20) which dominates the sum will be that associated with the paths for which ε_N is minimum. The minimizing path is the most probable low-temperature escape path. Because other terms can be neglected, the activation energy ε_A must equal the minimum ε_N. This equivalence of ε_A and the minimum ε_N is the relation that allows activation energies to be computed efficiently.

The physical interpretation of ε_N becomes apparent if we consider its dimensioned equivalent,

$$E_N=\tfrac{1}{4}\int_0^{t_e} I_N^2 R\, dt . \tag{22}$$

The maximum power that can be drawn from a current source I shunted by a resistance R is $\frac{1}{4}I^2R$, a quantity sometimes called the available power. Thus, E_N is the maximum energy available to the remainder of the circuit from the Johnson noise of the resistance. Using this terminology, we can state the minimum principle as follows. In the limit of low temperatures the most probable escape trajectory is that which requires the minimum available thermal-noise energy and this minimum energy is the activation energy of escape.

Although developed here with reference to a specific system, the principle of minimum available noise energy applies generally to problems in which noise-induced escape is due to white Gaussian noise derived from a linear dissipative element. The principle is applicable to systems having a wide range of dynamical properties because the only requirement on the equation of motion is that it establish a one-to-one correspondence between escape paths and noise waveforms. However, applicability depends strongly on the characteristics of the noise source. To ensure that the noise amplitudes at successive times are effectively uncorrelated, the noise spectrum must be white for frequencies up to and somewhat greater than the highest natural frequency of the noise-free system. To ensure that the average noise amplitudes follow a Gaussian distribution, it suffices that the noise process be a Gaussian process. Finally, to ensure the required relationship between noise and temperature, the noise must derive from a linear dissipative element to which the fluctuation-dissipation theorem applies. Because the noise associated with resistors in electrical systems and viscous damping in mechanical systems usually meet these requirements,[14] the principle of minimum available noise energy is expected to be widely useful.

Application of the minimum principle to the computation of activation energies proceeds through a search for the escape path that requires the minimum available

noise energy. This search is simplified by the fact that the minimum ε_N necessarily occurs for a path ending at a saddle point on the basin boundary. Because the basin boundary is formed by the insets of saddle points, a trajectory that meets the boundary at an arbitrary point can be extended to a saddle point along a path for which $i_N=0$. Thus, ε_N for an arbitrary end point can never be less than that for a path ending at a saddle point. The search for the path with minimum ε_N can thus be restricted to those ending at saddle points. The starting point of the minimizing trajectory can also be chosen in advance even when the attractor is not a fixed point. All points of the attractor are equally suitable as starting points because noise energy is not required for the system to move between them. Thus, in searching for the escape path requiring the minimum available noise energy, the possible end points of the path are predetermined and a starting point on the attractor can be selected arbitrarily without loss of generality.

The search for a trajectory that minimizes ε_N is carried out by application of the calculus of variations. An expression for ε_N specific to the dc-biased Josephson junction is obtained by combining Eqs. (1) and (21),

$$\varepsilon_N=\tfrac{1}{4}\int_0^{t_e}(\beta\ddot{\phi}+\dot{\phi}+\sin\phi-i_0)^2dt \ . \tag{23}$$

Because $[\phi(0),\dot{\phi}(0)]$ and $[\phi(t_e),\dot{\phi}(t_e)]$ are fixed, the calculus of variations can be applied to derive an equation for the trajectories that lead to stationary values of ε_N,

$$\beta^2\dddot{\phi}+(2\beta\cos\phi-1)\ddot{\phi}-\beta\dot{\phi}^2\sin\phi+(\sin\phi-i_0)\cos\phi=0 \ . \tag{24}$$

This equation is to be solved subject to the boundary conditions that $[\phi(0),\dot{\phi}(0)]$ is a point on the attractor and $[\phi(t_e),\dot{\phi}(t_e)]$ is a saddle point. Once a solution is found, the noise current can be derived from Eq. (1) and used to compute the corresponding ε_N. For a given t_e and fixed boundary conditions, there are generally several solutions to Eq. (24), corresponding to various local and global minima and maxima in ε_N. Assuming for the moment that the global minimum can be found for any given t_e, the minimum of ε_N over all escape paths is obtained by taking the limit as t_e goes to infinity. The necessity of taking this limit derives from the fact that the duration of an escape path can always be extended without increasing ε_N simply by adding an initial interval during which $i_N=0$ and the system remains on the attractor. Thus, the minimum ε_N for long escape times can never be greater than that for short times and the increased flexibility permitted by a longer escape time can be expected to decrease the minimum ε_N. The principle of minimum available noise energy ensures that the minimum ε_N found in this way is the activation energy for escape.

The greatest practical difficulty encountered in application of the minimum principle to calculating ε_A is that of determining whether a given solution of Eq. (24) corresponds to the global minimum of ε_N for the assumed t_e. Because ε_N can be directly evaluated for any escape path, it is easy to determine which of several solutions is a candidate for the global minimum, but the possibility that a solution with lower ε_N remains undiscovered cannot be easily ruled out. Fortunately, the simple strategies described in the following sections for finding solutions of minimum ε_N are usually effective in locating the global minimum for a given t_e. Taking the limit of this minimum ε_N as $t_e\to\infty$ is also practical because convergence to an asymptotic value is usually rapid. Thus, although there are uncertainties associated with calculation of ε_A through the minimum principle, an accurate value is often obtained directly and efficiently by variational methods.

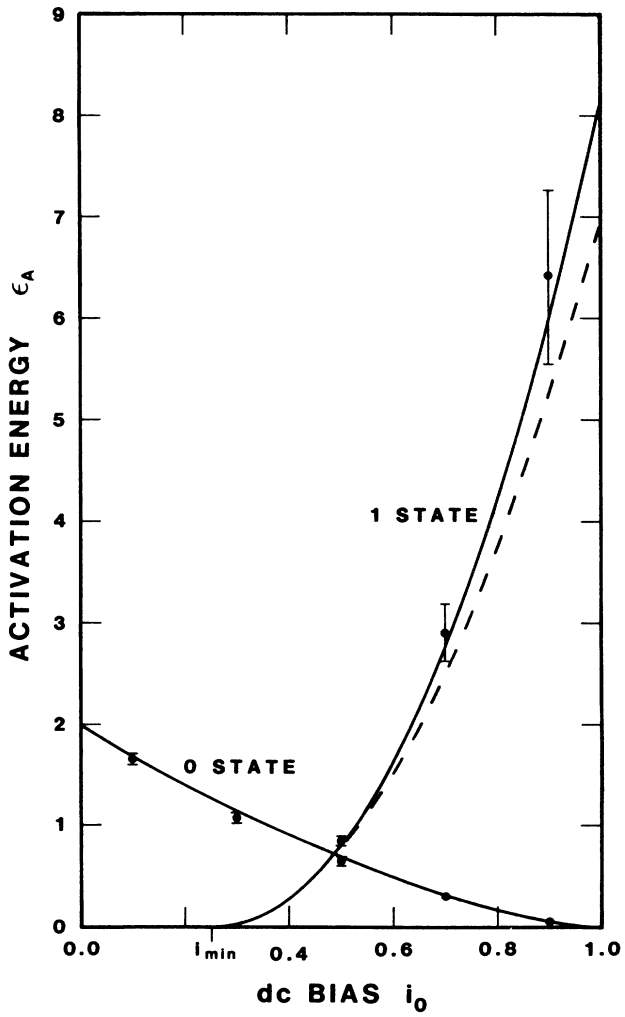

FIG. 6. Activation energy (units of $\hbar I_c/2e$) for thermally induced escape from the 0 state and 1 state as a function of dc bias for $\beta=25$. Circles indicate values obtained through Monte Carlo simulations and solid lines indicate the results obtained through application of the principle of minimum available noise energy. The dashed curve is the analytic approximation given by Eq. (42) with $i_{\min}=0.2521$.

The basic validity of calculating activation energies through the minimum principle is demonstrated by Figs. 6 and 7 which summarize the results of this paper. Here activation energies for escape from the 0 state and 1 state are plotted as a function of dc bias for β values of 25 and 4. The results of Monte Carlo simulations are shown by

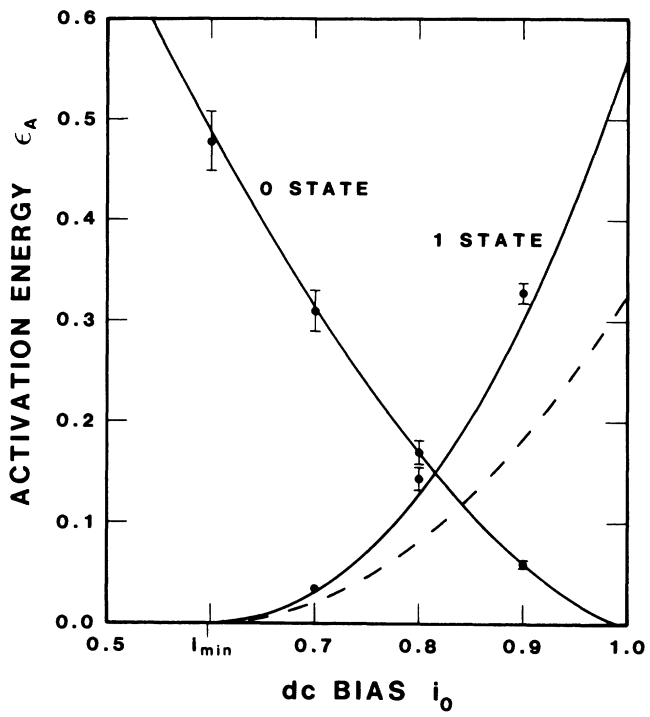

FIG. 7. Activation energy for thermally induced escape from the 0 state and 1 state as a function of dc bias for $\beta=4$. Circles indicate values obtained through Monte Carlo simulations and solid lines indicate the results obtained through application of the principle of minimum available noise energy. The dashed curve is the analytic approximation given by Eq. (42) with $i_{\min}=0.5974$.

solid circles with error bars selected, as previously discussed, to indicate the accuracy of fit to the Arrhenius form. Solid lines plot the values obtained by application of the minimum principle. Because the two methods of calculation are theoretically equivalent, the observed agreement is not surprising. The agreement does, however, establish that the variational methods used are effective in locating the trajectory corresponding to the global minimum of the available noise energy required for escape. The data presented in Figs. 6 and 7 will be discussed further as we describe these methods in detail in the following sections.

IV. POTENTIAL WELL

Escape from the 0 state corresponds to the case of escape from a potential well. For this case the activation energy is known to be the difference in potential energy between the saddle point and the attractor and the most probable escape path is known to be the time reversal of the trajectory by which the system relaxes from the saddle point to the attractor. Knowledge of these exact results makes escape from the 0 state an ideal test case for calculations based on the minimum principle.

Expressions for the mean escape time for thermally induced escape from the 0 state have been derived for a variety of limiting cases.[18–25] The result obtained by applying the theory of Kramers[3] for the low-temperature limit ($\Gamma \ll \Delta U$ and $\Gamma < 2\pi\Delta U/[\beta(1-i_0^2)^{1/2}]^{1/2}$) is

$$\tau=\frac{4\pi\beta}{[1+4\beta(1-i_0^2)^{1/2}]^{1/2}-1}\exp(\Delta U/\Gamma)\ , \tag{25}$$

where ΔU is the depth of the potential well

$$\begin{aligned}\Delta U &= U(\phi_{\max})-U(\phi_{\min}) \\ &= 2(1-i_0^2)^{1/2}+2i_0\sin^{-1}i_0-\pi\,|\,i_0\,|\ .\end{aligned} \tag{26}$$

Because the activation energy is defined by the asymptotic low-temperature form of τ, Eq. (25) confirms that $\varepsilon_A=\Delta U$ and Eq. (26) gives an explicit formula for ε_A.

Equation (25) also provides a check on our Monte Carlo results for τ. A comparison between Monte Carlo data and Eq. (25) is made in Fig. 5 where the analytic result is plotted as a dashed line. Although agreement is good at low temperatures, small but significant differences are found for the high-temperature data points. This discrepancy may result because Γ is not sufficiently less than ΔU for Eq. (25) to be accurate at the higher temperatures. Whatever their origin, the observed differences are small enough that the accuracy of our Monte Carlo simulations is largely confirmed by comparison with the analytic result.

The fact that the most probable escape trajectory for a potential well is the time reversal of the trajectory by which the system relaxes from the saddle point to the attractor can be shown by direct application of the minimum principle. The relaxation trajectory is a limiting case of a function $\phi_R(t)$ defined on the interval $(0,T)$. $\phi_R(t)$ is the path followed by the noise-free system for the initial conditions $[\phi_R(0),\dot{\phi}_R(0)]=[\phi_{\max},\delta]$ where δ is a small velocity which starts the system moving from the saddle point toward the attractor of interest. Because ϕ_R is a trajectory of the noise-free system, it satisfies the equation

$$\beta\ddot{\phi}_R+\dot{\phi}_R+U'(\phi_R)=0\ . \tag{27}$$

If the time T is taken to be sufficiently large for a given δ the endpoint of the trajectory will approach the attractor arbitrarily closely. In the limit $\delta\to 0$ and $T\to\infty$, $\phi_R(t)$ becomes the relaxation trajectory. Similarly, the reverse relaxation trajectory is obtained from the function

$$\phi_E(t)=\phi_R(T-t)\ , \tag{28}$$

in the limit $\delta\to 0$ and $T\to\infty$. This path begins at the fixed point and ends at the saddle point and thus represents a possible escape trajectory. The noise current needed to drive the system along ϕ_E is defined by

$$\beta\ddot{\phi}_E+\dot{\phi}_E+U'(\phi_E)=i_N \tag{29}$$

and the required available noise energy is

$$\begin{aligned}\varepsilon_N &= \tfrac{1}{4}\int_0^T i_N^2\,dt \\ &= \tfrac{1}{4}\int_0^T[\beta\ddot{\phi}_E+\dot{\phi}_E+U'(\phi_E)]^2\,dt\ .\end{aligned} \tag{30}$$

Using Eq. (28), we can express ε_N in terms of ϕ_R as

$$\varepsilon_N=\tfrac{1}{4}\int_0^T\left[\beta\frac{d^2}{dt^2}[\phi_R(T-t)]+\frac{d}{dt}[\phi_R(T-t)]+U'[\phi_R(T-t)]\right]^2dt$$
$$=\tfrac{1}{4}\int_0^T\{\beta\ddot{\phi}_R(t')-\dot{\phi}_R(t')+U'[\phi_R(t')]\}^2dt' , \quad (31)$$

where we have made the substitution $t'=T-t$. Finally, substituting for the quantity $\beta\ddot{\phi}_R+U'(\phi_R)$ using Eq. (27) and removing the prime from the integration variable yields

$$\varepsilon_N=\int_0^T\dot{\phi}_R^2dt . \quad (32)$$

Because $\dot{\phi}^2$ is the power dissipated in the resistance, the above time integral is the total energy dissipated over the trajectory ϕ_R. This energy, the energy dissipated in the process of relaxation in a noise-free system, must equal the difference in stored energy (kinetic plus potential) between the initial and final states. Because the initial and final states approach $(\phi_{\max},0)$ and $(\phi_{\min},0)$, respectively, in the limit that ϕ_R approaches the relaxation trajectory, we conclude that for the limiting path,

$$\varepsilon_N=U(\phi_{\max})-U(\phi_{\min}) . \quad (33)$$

This equation is the anticipated result: the available noise energy required to execute the relaxation trajectory in reverse equals the depth ΔU of the potential well. There can be no escape trajectory with a smaller ε_N because energy conservation requires that at least this amount of energy be drawn from the resistivity shunted noise source in order to move the system from the attractor to the saddle point. Thus, the reverse relaxation trajectory minimizes ε_N and by the minimum principle is the most probable low-temperature escape trajectory. Because this conclusion does not depend on the form of the potential, the most probable escape path is the reverse relaxation trajectory in all potential systems.

A further understanding of the available noise energy ε_N can be gained by comparing it with the energy ε_I drawn from the bare noise source and the energy ε_R dissipated in the resistance. By its definition, Eq. (21), ε_N is the maximum energy available to the remainder of the circuit from the terminals of the resistively shunted noise source. Thus, ε_N is an upper limit on the energy transferred to the capacitance, Josephson element, and dc-bias source (or, in the language of a particle in a well, to kinetic and potential energy) during the escape process. ε_I and ε_R, defined by

$$\varepsilon_I=\int_0^{t_e}i_N\dot{\phi}\,dt \quad (34)$$

and

$$\varepsilon_R=\int_0^{t_e}\dot{\phi}^2dt , \quad (35)$$

are the energy drawn from the bare noise source and the energy dissipated in the resistance, respectively. The energy drawn from the shunted noise source is thus $\varepsilon_I-\varepsilon_R$ and in the general case this quantity is bounded by ε_N so that

$$\varepsilon_I-\varepsilon_R\le\varepsilon_N . \quad (36)$$

In the case of escape from a potential well along the reverse relaxation trajectory, we have shown that $\varepsilon_N=\Delta U$ and ΔU is the actual energy supplied to the remainder of the circuit from the shunted noise source. Thus, for this case $\varepsilon_I-\varepsilon_R$ is not just bounded by ε_N but equal to it. Furthermore, ε_R can be evaluated explicitly for the reverse relaxation trajectory by again considering this path as a limit of ϕ_E,

$$\varepsilon_R=\int_0^T\dot{\phi}_E^2dt=\int_0^T\left[\frac{d}{dt}[\phi_R(T-t)]\right]^2dt=\int_0^T\dot{\phi}_R^2dt=\Delta U . \quad (37)$$

For escape from a potential well along the most probable path, we conclude that $\varepsilon_N=\varepsilon_R=\Delta U$ and $\varepsilon_I=2\Delta U$. That is, of the energy provided by the bare noise source in the process of moving the system from the attractor to the saddle point, half is dissipated in the shunt resistance and half is stored as potential energy. The case of escape from a potential well is thus special in that the activation energy ε_A can equivalently be considered as the depth of the well ΔU or any of the three quantities ε_N, ε_R, or $\varepsilon_I/2$ associated with the most probable escape path. As will be shown in the following section, the activation energy for nonequilibrium escape problems is generally given by only one of these four quantities: the available noise energy ε_N associated with the most probable escape path.

In the remainder of this section we consider the problem of computing the escape path requiring minimum available noise energy by application of variational methods. For a given escape time t_e, the task is to solve Eq. (24) for a trajectory $\phi(t)$ which satisfies the boundary conditions that $[\phi(0),\dot{\phi}(0)]=[\phi_{\min},0]$ and $[\phi(t_e),\dot{\phi}(t_e)]=[\phi_{\max},0]$. That is, we seek a solution to Eq. (24) which begins at the attractor and ends at the saddle point. Because Eq. (24) is fourth order, integration can be started from $t=0$ only if $\phi(0)$, $\dot{\phi}(0)$, $\ddot{\phi}(0)$, and $\dddot{\phi}(0)$ are specified. While $\phi(0)$ and $\dot{\phi}(0)$ are fixed by the boundary conditions, $\ddot{\phi}(0)$ and $\dddot{\phi}(0)$ must be determined through a process of trial and error such that the values of $\phi(t_e)$ and $\dot{\phi}(t_e)$ obtained by integrating Eq. (24) from 0 to t_e meet the boundary conditions at t_e. Finding such values for $\ddot{\phi}(0)$ and $\dddot{\phi}(0)$ determines an escape trajectory for which ε_N is stationary and possibly minimal.

The numerical technique used to solve for $\ddot{\phi}(0)$ and $\dddot{\phi}(0)$ is Newton's method for finding the zeros of a function. Because $\phi(0)$ and $\dot{\phi}(0)$ are fixed, the process of integrating Eq. (24) from 0 to t_e may be thought of as defining two functions, F and G, such that

$$\phi(t_e)-\phi_{\max}=F[\ddot{\phi}(0),\dddot{\phi}(0)] , \quad (38)$$

$$\dot{\phi}(t_e)=G[\ddot{\phi}(0),\dddot{\phi}(0)] . \quad (39)$$

In terms of F and G, the problem to be solved reduces to finding values of $\ddot{\phi}(0)$ and $\dddot{\phi}(0)$ for which $F=G=0$, that

is, to finding the simultaneous zeros of F and G. If we denote $\dot{\phi}(0)$ by x and $\ddot{\phi}(0)$ by y then Newton's method proceeds by evaluating F, G, and the partial derivatives F_x, F_y, G_x, and G_y at some initial guess, x_1 and y_1, for the simultaneous zeros. Linear extrapolation based on this information can be used to predict more accurate values, x_2 and y_2, for the simultaneous zeros,

$$x_2 = x_1 + \left[\frac{GF_y - FG_y}{F_x G_y - G_x F_y} \right]_{(x,y)=(x_1,y_1)}, \tag{40}$$

$$y_2 = y_1 + \left[\frac{FG_x - GF_x}{F_x G_y - G_x F_y} \right]_{(x,y)=(x_1,y_1)}. \tag{41}$$

These equations can be applied repeatedly by using the last values of x_2 and y_2 as the next values for x_1 and y_1 to obtain even more accurate simultaneous zeros. If the initial guess is reasonably good, a few iterations are usually sufficient to yield values for $\dot{\phi}(0)$ and $\ddot{\phi}(0)$ that define a trajectory satisfying the specific boundary conditions to a high degree of accuracy. Each iteration requires the numerical evaluation of F and G and their first derivatives at (x_1,y_1). These quantities can be computed by integrating Eq. (24) three times with initial values for $\ddot{\phi}$ and $\dddot{\phi}$ set first to x_1 and y_1, then to $x_1+\Delta x$ and y_1, and finally to x_1 and $y_1+\Delta y$, where Δx and Δy are small increments.

A less certain step in the variational procedure is the search for the particular solution to Eq. (24) corresponding to the global minimum of ε_N. A strategy that often proves successful begins by considering an escape time t_e that is somewhat less than the natural response times of the system. In this limit Newton's method usually converges to an accurate solution even when the first guess for $\dot{\phi}(0)$ and $\ddot{\phi}(0)$ is very approximate. The type of escape trajectory to be sought initially is one that connects the attractor and saddle point as directly as possible. An interactive program that plots solutions of Eq. (24) can usually be used to locate an approximate escape trajectory of this type by applying trial and error to the selection of $\dot{\phi}(0)$ and $\ddot{\phi}(0)$. Newton's method is then applied to find a solution which satisfies the boundary conditions accurately. Presuming that this solution minimizes ε_N for a given t_e, we wish to extend it to escape times that exceed the natural response times of the system. Because Newton's method generally requires a more accurate initial guess when t_e is large, the process of extending t_e is best accomplished in small increments, using the accurate values of $\dot{\phi}(0)$ and $\ddot{\phi}(0)$ obtained for the last t_e as an initial guess for the next larger t_e. As t_e is increased, the escape path is expected to relax toward a trajectory that minimizes ε_N.

As an example of this procedure, we consider escape from the 0 state for the situation pictured in Fig. 4. By solving Eq. (24) for a series of escape times, we obtain the trajectories shown in Fig. 8. The result for $t_e=10$ is a necessarily rapid transition from $\phi_{\min}$ to $\phi_{\max}$. As t_e is increased, the transition becomes more gradual at first but for t_e greater than about 40 the transition is virtually fixed in shape and further increases in t_e merely extend the dwell time near $\phi_{\min}$ and $\phi_{\max}$. The values of ε_N for this series of trajectories are 8.905, 1.843, 1.275, 1.211, 1.206, and 1.206 for t_e values spanning the range from 10 to 60 in increments of 10. Convergence to a definite

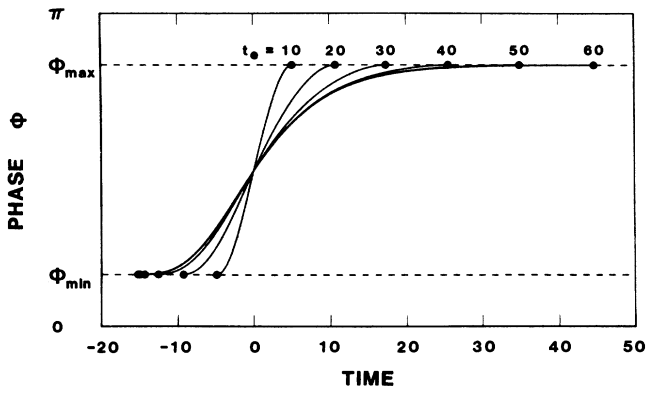

FIG. 8. Phase as a function of time for a series of escape trajectories obtained by solving Eq. (24) for different escape times t_e. Trajectories are for escape from the 0 state in the case $\beta=25$ and $i_0=0.5$. For ease of comparison, the time origin of each trajectory has been shifted to the point at which $\phi=\pi/2$. Dots indicate the initial and final points of each trajectory.

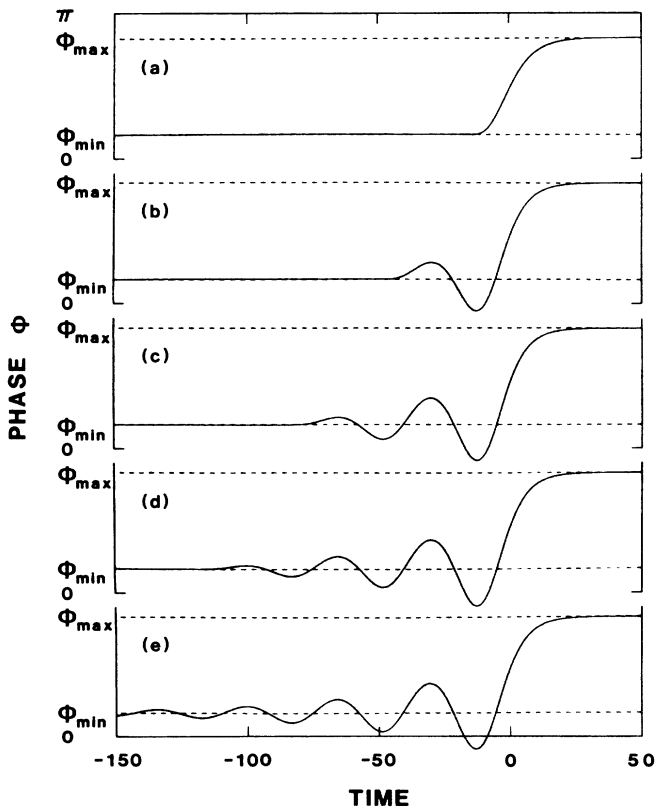

FIG. 9. Phase as a function of time for a sequence of four oscillatory escape trajectories solving Eq. (24) [(a)–(d)] and for the reverse relaxation trajectory (e). All trajectories are for escape from the 0 state in the case $\beta=25$ and $i_0=0.5$. The time origin for each trajectory has been shifted to the point at which $\phi=\pi/2$.

value for ε_N thus occurs rapidly with increasing t_e and we may hope to have discovered the global minimum for ε_N through this procedure.

However, for the case at hand there are escape trajectories having even smaller ε_N than the nearly direct path pictured in Fig. 8. Because the system is underdamped, less available noise energy is required for escape if it is applied with a periodicity that matches the natural oscillation frequency of the system to gradually build the amplitude of oscillation until escape occurs. By seeking a nearly direct escape path, we have overlooked the class of oscillatory escape paths that includes the actual minimizing trajectory. Beginning again with trial and error choices for $\dot{\phi}(0)$ and $\ddot{\phi}(0)$, we find that such oscillatory solutions are easily obtained and can be arranged in sequence according to the number of oscillations that occur before the saddle point is reached. Four solutions from this sequence are shown in frames (a)–(d) of Fig. 9. Each of these trajectories is plotted in the limit that $t_e \to \infty$ and the values of ε_N corresponding to frames 9(a)–9(d) are 1.206, 0.773, 0.705, and 0.690. These solutions of Eq. (24) are to be compared with the reverse relaxation trajectory shown in frame 9(e) for which ε_N is 0.685. The close similarity between frame 9(d) and the exact result of frame 9(e) confirms that the most probable escape trajectory can be obtained through variational methods. The value of ε_N for the trajectory shown in frame 9(d) also agrees with the exact result within 1%, confirming that the variational method is a viable technique for the calculation of activation energies. Indeed, the variational results for ε_A plotted in Figs. 6 and 7 for the 0 state agree everywhere with the exact result given by Eq. (26) within the accuracy of the figure.

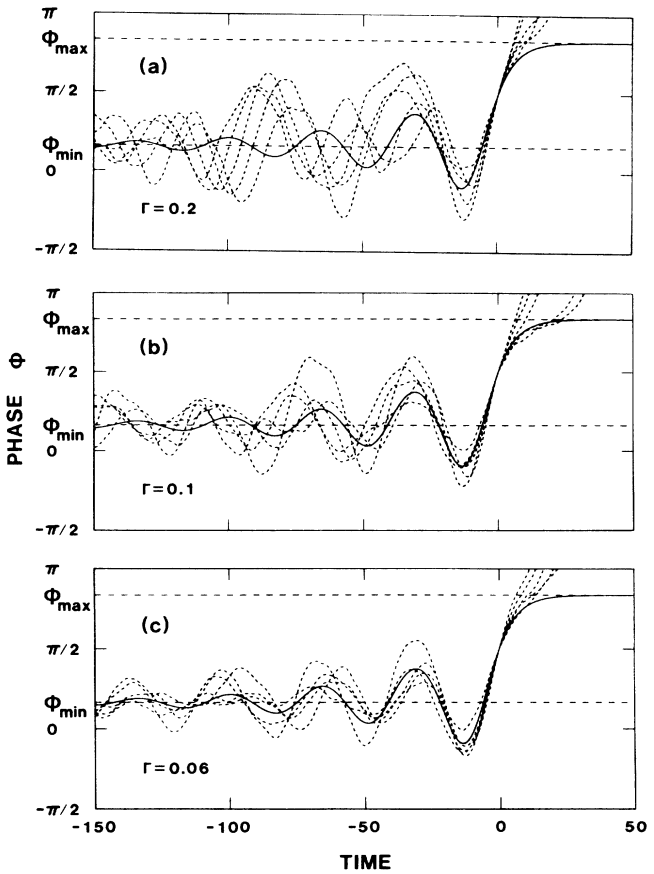

FIG. 10. Phase as a function of time for Monte Carlo escape routes from the 0 state calculated for (a) $\Gamma=0.2$, (b) $\Gamma=0.1$, and (c) $\Gamma=0.06$. The system parameters are $\beta=25$ and $i_0=0.5$. Each frame shows five Monte Carlo escape routes (dashed lines) and the reverse relaxation trajectory (solid line). The time origin for each trajectory has been shifted to the point at which $\phi=\pi/2$.

Although the variational method is primarily of interest for evaluation of activation energies, it yields as a by-product the most probable low-temperature escape path. The significance of this path is illustrated in Fig. 10 which compares Monte Carlo escape routes computed at three temperatures with the reverse relaxation trajectory. We have argued that the probability of a given escape route is proportional to the product of a prefactor and an exponential factor $\exp(-\varepsilon_N/\Gamma)$ where ε_N is the available noise energy required to execute the route. If the prefactors are weakly temperature dependent, the most probable escape route in the limit of low temperature is that with the smallest ε_N, namely $\varepsilon_N=\varepsilon_A$. At any finite temperature Γ, however, all of the escape paths having ε_N within Γ of ε_A will occur with comparable probability, assuming their prefactors are not too different. Thus, as the temperature is increased, the range of escape paths likely to be observed also increases. As the temperature is decreased, the observed escape paths will be restricted to those close to the path with smallest ε_N. This effect is illustrated in Fig. 10. Here we plot the Monte Carlo escape trajectories over a brief interval of time including the time at which escape occurs. Each frame shows a sample of five Monte Carlo trajectories computed for a given Γ (dashed lines) together with the reverse relaxation trajectory (solid line). In frame 10(a), for which $\Gamma/\varepsilon_A=0.29$, the oscillations that precede escape in the Monte Carlo simulations bear little resemblance to those of the reverse relaxation trajectory except for the single dip occurring just before the escape event. In frames 10(b) and 10(c), for which $\Gamma/\varepsilon_A=0.15$ and 0.088, respectively, the correlation between the Monte Carlo trajectories and the reverse relaxation trajectory is distinctly stronger, with rough agreement over a period of several oscillations at the lowest temperature. This agreement confirms that the escape path requiring the least available noise energy, the reverse relaxation trajectory in this case, has physical significance as the limiting path for escape at low temperatures.

V. BASIN OF ATTRACTION

The general case of thermally induced escape from a basin of attraction is represented here by the problem of escape from the 1 state. The 1 state of the noise-free Josephson junction is a stable nonequilibrium state in which energy is constantly supplied to the system by the dc bias and dissipated in the resistance. Because the 1 state is not an equilibrium state, the classical analysis of Kramers[3] for thermally induced escape is not applicable.

In recent years, however, escape from the 1 state has been studied by several authors using a variety of methods appropriate to nonequilibrium systems.[24,26–31] In this section we apply the principle of minimum available noise energy to determine the activation energy for escape from the 1 state. Our results are compared with both Monte Carlo simulations and previous calculations.

The variational approach to finding the most probable escape trajectory proceeds for the 1 state as for the 0 state by seeking solutions of Eq. (24). In this case the initial condition is that the trajectory begins at a point on the periodic attractor rather than the fixed point. As for escape from the 0 state, the trajectory must end at the saddle point. Because the natural response of the system in the neighborhood of the periodic attractor is not oscillatory, as was shown in Sec. II, we anticipate that the minimizing trajectory will connect the attractor and the saddle point nearly directly. This expectation proves to be justified and eliminates the need to explore a class of oscillatory solutions as in the case of the 0 state. However, one additional search strategy does appear to be required for the 1 state. The problem is related to the relaxation of the trajectory toward a minimizing solution as the escape time t_e is extended. This relaxation proves to be incomplete if solutions are always obtained by searching for values of $\ddot{\phi}(0)$ and $\dddot{\phi}(0)$ which yield the correct values of $\phi(t_e)$ and $\dot{\phi}(t_e)$. An alternative is to integrate Eq. (24) backward in time from t_e to 0, beginning the integration with values of $\phi(t_e)$ and $\dot{\phi}(t_e)$ specified by the boundary condition and values of $\ddot{\phi}(t_e)$ and $\dddot{\phi}(t_e)$ chosen by trial and error. In this case, a solution is obtained when the selected values of $\ddot{\phi}(t_e)$ and $\dddot{\phi}(t_e)$ yield an initial state $[\phi(0),\dot{\phi}(0)]$ falling on the periodic attractor. Extending t_e by forward integration allows greater flexibility in the form of the trajectory near the saddle point while backward integration allows greater flexibility near the attractor. Using a combination of both procedures yields apparently complete relaxation to the minimizing trajectory.

An example of an escape trajectory for the 1 state that was obtained by solving Eq. (24) is shown in Fig. 11 for the case $\beta=25$ and $i_0=0.5$. For this trajectory the escape time is $t_e=100$ and the required available noise energy, $\varepsilon_N=0.81$, is thought to be nearly minimal. Thus, the trajectory shown in Fig. 11 is expected to be close to the most probable escape path. If the problem were that of escape from a potential well, the most probable escape path would coincide with the time reversal of the outset trajectory connecting the saddle point with the attractor. This outset trajectory is shown for the case at hand in Fig. 4(b). Comparison of the two figures reveals that the most probable escape trajectory is entirely different from the reverse outset trajectory. Although the two trajectories are similar in shape near the attractor, the reverse outset flows in a direction opposite to the most probable escape path. In fact, the reverse outset trajectory re-

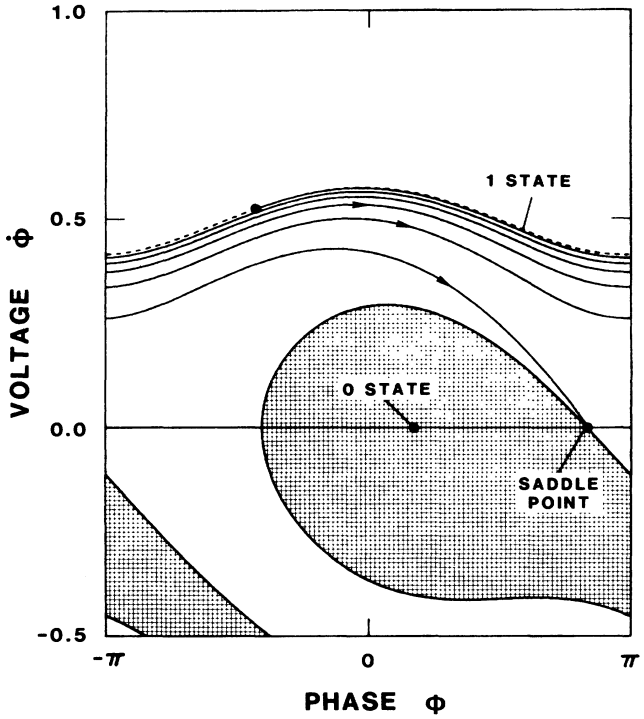

FIG. 11. State-space diagram of an escape trajectory for the 1 state obtained by solving Eq. (24) for $\beta=25$, $i_0=0.5$, and $t_e=100$. The escape trajectory is shown by a solid line and the periodic trajectory corresponding to the 1 state is shown by a dashed line. The crosshatched region is the basin of attraction of the 0 state.

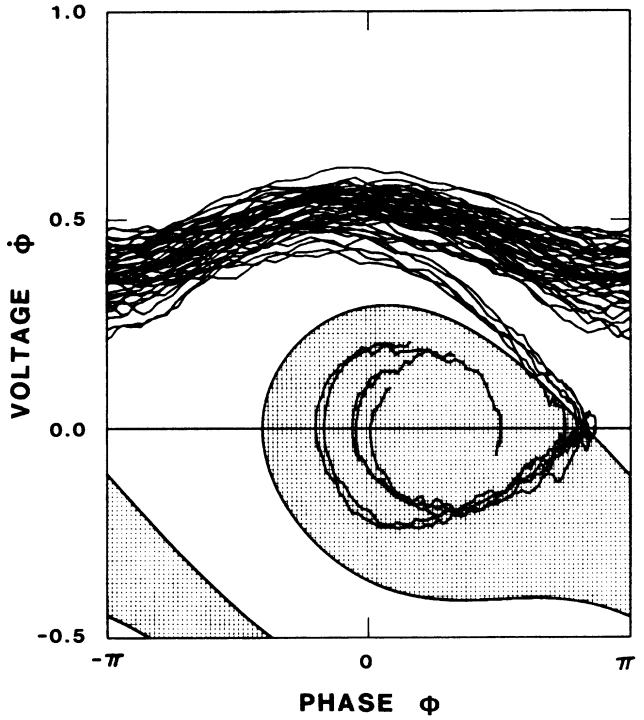

FIG. 12. State-space diagram of Monte Carlo escape trajectories for the 1 state. Five trajectories are shown for the case $\beta=25$, $i_0=0.5$, and $\Gamma=0.08$. Each trajectory is plotted over an interval of 190 time units spanning the time at which escape occurred. The crosshatched region is the basin of attraction of the 0 state.

quires infinite available noise energy for its execution because it follows the attractor in reverse for an infinite time. Thus, when the attractor is a limit cycle rather than a fixed point, escape paths which approximate the reverse relaxation trajectory are extremely unlikely.

Monte Carlo simulations confirm that the escape path shown in Fig. 11 is close to the most probable path. Five Monte Carlo escape paths are plotted in Fig. 12 for a temperature at which $\Gamma/\varepsilon_A \approx 0.1$. As in the case of escape from the 0 state, agreement between the Monte Carlo paths and the path of minimum ε_N is most apparent near the saddle point. All five of the Monte Carlo trajectories approach the basin boundary at the same shallow angle as the path shown in Fig. 11 and cross the boundary near the saddle point. Thus, the variational procedure yields an approximation to the most probable escape trajectory which is consistent with Monte Carlo simulations.

The relationship between ε_N, ε_I, and ε_R for the most probable escape path is also different for nonequilibrium escape problems. In Sec. IV we showed that in the general case $\varepsilon_I - \varepsilon_R \leq \varepsilon_N$ but for the most probable escape path in potential problems $\varepsilon_I - \varepsilon_R = \varepsilon_N$ and, more specifically, $\varepsilon_N = \varepsilon_R = \varepsilon_I/2$. For escape from the 1 state in the case $\beta = 25$ and $i_0 = 0.5$, the energies associated with the most probable path are $\varepsilon_N \approx 0.8$, $\varepsilon_I \approx -4$, and $\varepsilon_R = \infty$. In this case, the relation $\varepsilon_I - \varepsilon_R \leq \varepsilon_N$ is satisfied not by equality but by extreme inequality. Although a small amount of energy, $\varepsilon_N \approx 0.8$, could be drawn from the shunted noise source during the escape process, energy is actually absorbed by both the bare noise source, $\varepsilon_I \approx -4$, and by the resistance, $\varepsilon_R = \infty$. The absorption of energy makes sense, given that the 1 state corresponds to a particle moving down an incline at its terminal velocity, because the particle must be brought to a stop during the escape process. The fact that $\varepsilon_I \approx -4$ is thus a reflection of the fact that the noise source acts as brake. The fact that $\varepsilon_R = \infty$ is related to the fact that the minimizing trajectory is one for which in the limit $t_e \to \infty$ infinite time is spent initially in the neighborhood of the periodic attractor. Because energy is constantly dissipated in the resistance during this initial dwell time, $\varepsilon_R \to \infty$ as $t_e \to \infty$. The important point here is that ε_I and ε_R have no simple relationship to ε_N for nonequilibrium problems. Thus, in the general case, the activation energy is equal to the minimum value of ε_N but unrelated to the values of ε_I and ε_R for the minimizing trajectory.

The relevance of the available noise energy to thermally induced escape is in a sense surprising. On an intuitive basis, we might anticipate that the most probable escape path would be one that minimizes an actual energy transfer, either the energy drawn from the bare noise source ε_I or that drawn from the shunted noise source $\varepsilon_I - \varepsilon_R$, rather than an energy that is merely potentially available. In the case of escape from a potential well, the most probable escape path does in fact minimize the energy drawn from the bare noise source as well as the available noise energy. However, as the example above illustrates, escape from an attractor of a nonequilibrium system may require the removal of energy from the noise-free system rather than the addition of energy. The significance of the available noise energy to thermally induced escape results because it is a measure of noise strength that is independent of whether the noise adds to or subtracts from the energy of the system.

The accuracy with which variational calculations determine the activation energy for escape from the 1 state is confirmed by the data shown in Figs. 6 and 7. These figures compare activation energies computed in three ways: by variational methods which determine the trajectory requiring the minimum ε_N (solid lines), by direct Monte Carlo simulations (circles), and by an approximate analytic formula (dashed lines). The analytic formula, due to Ben-Jacob *et al.*,[26]

$$\varepsilon_A = \frac{\beta}{2}(i_0 - i_{\min})^2 , \tag{42}$$

is expected to be accurate in the limit of large β and small i_0. This formula for ε_A yields values that are about 90% of the variational result for $\beta = 25$ (Fig. 6) and about 60% for $\beta = 4$. These differences are consistent with the fact that Eq. (42) is accurate only in the limit of large β. However, because correction terms to the formula are of unknown order, Eq. (42) provides no specific bound on the accuracy of the variational results. Such a bound is provided by the Monte Carlo simulations which agree with the variational results within the assigned error limits in almost every case. This agreement confirms the accuracy of the variational method within about 10%.

A value for the activation energy for escape from the 1 state has been obtained numerically by Graham and Tél using another method. These authors find[32] an ε_A of 14.7 for the case $\beta = (0.13)^{-2} \approx 59.2$ and $i_0 = 0.83$. Applying the analytic formula ($i_{\min} = 0.1648$), Monte Carlo simulations, and the variational method to this case, we obtain values for ε_A of 13.1, 14.5 ± 1.0, and 14.4, respectively. For this high-β case, all four calculations are in basic agreement, with a difference of only 2% between our variational result and the value of Graham and Tél.

Application of the principle of minimum available noise energy to the problem of thermally induced escape from the 0 state and 1 state of the dc-biased Josephson junction demonstrates that the principle can be used as a basis for the practical computation of activation energies and most probable escape trajectories. Although the problem of escape from the 0 state is one that can be solved analytically in the low-temperature limit, accurate activation energies for the 1 state in the presence of moderate damping were obtained here for the first time by a method other than Monte Carlo simulation. Previous work[11] has demonstrated that the variational method can be extended to more complex situations, including escape from a chaotic attractor in a three-dimensional state space. The simplicity and generality of calculations based on the principle of minimum available noise energy suggest that the method will prove valuable in estimating the stability of steady-state solutions for a wide range of nonequilibrium systems.

ACKNOWLEDGMENTS

The author thanks E. Ben-Jacob for correspondence pointing out the relevance of the prior work of Freidlin and Ventsel' to the principle of minimum available noise energy. The present work was supported in part by the U.S. Office of Naval Research under Contract No. N00014-88-F-0018.

[1]R. Landauer, Phys. Today **31** (11), 23 (1978).
[2]R. L. Kautz, J. Appl. Phys. **62**, 198 (1987).
[3]H. A. Kramers, Physica **7**, 284 (1940); R. Landauer and J. A. Swanson, Phys. Rev. **121**, 1668 (1961).
[4]P. Hanggi, J. Stat. Phys. **42**, 105 (1986).
[5]A. D. Ventsel' and M. I. Freidlin, Russian Math. Surveys **25**, 1 (1970).
[6]D. Ludwig, SIAM Rev. **17**, 605 (1975).
[7]B. J. Matkowsky and Z. Schuss, SIAM J. Appl. Math. **33**, 365 (1977).
[8]M. I. Freidlin and A D. Wentzell, *Random Perturbations of Dynamical Systems* (Springer, New York, 1984).
[9]R. Graham, in *Stochastic Nonlinear Systems,* edited by L. Arnold and R. Lefever (Springer, New York, 1981).
[10]R. Graham and T. Tél, Phys. Rev. A **31**, 1109 (1985).
[11]R. L. Kautz, Phys. Lett. A **125**, 315 (1987).
[12]W. C. Stewart, Appl. Phys. Lett. **12**, 277 (1968).
[13]D. E. McCumber, J, Appl. Phys. **39**, 3113 (1968).
[14]D. Middleton, *An Introduction to Statistical Communication Theory* (McGraw-Hill, New York, 1960), Chap. 11.
[15]E. A. Coddington and N. Levinson, *Theory of Ordinary Differential Equations* (McGraw-Hill, New York, 1955), Chap. 3.
[16]R. L. Kautz and R. Monaco, J. Appl. Phys. **57**, 875 (1985).
[17]A. J. Lichtenberg and M. A. Lieberman, *Regular and Stochastic Motion* (Springer, New York, 1983), Chap. 7.
[18]Y. M. Ivanchenko and L. A. Zil'berman, Pis'ma Zh. Eksp. Teor. Fiz. **8**, 189 (1968) [Sov. Phys.—JETP Lett. **8**, 113 (1968)]; Zh. Eksp. Teor. Fiz. **55**, 2395 (1968) [Sov. Phys.—JETP **28**, 1272 (1969)].
[19]V. Ambegaokar and B. I. Halperin, Phys. Rev. Lett. **22**, 1364 (1969).
[20]M. J. Stephen, Phys. Rev. **186**, 393 (1969).
[21]A. C. Biswas and S. S. Jha, Phys. Rev. B **2**, 2543 (1970).
[22]P. A. Lee, J. Appl. Phys. **42**, 325 (1971).
[23]M. Büttiker, E. P. Harris, and R. Landauer, Phys. Rev. B **28**, 1268 (1983).
[24]V. I. Mel'nikov, Zh. Eksp. Teor. Fiz. **88**, 1429 (1985) [Sov. Phys.—JETP **61**, 855 (1985)].
[25]R. Cristiano and P. Silvestrini, J. Appl. Phys. **60**, 3243 (1986).
[26]E. Ben-Jacob, D. J. Bergman, B. J. Matkowsky, and Z. Schuss, Phys. Rev. A **26**, 2805 (1982).
[27]H. D. Vollmer and H. Risken, Z. Phys. B **52**, 159 (1983).
[28]P. Jung and H. Risken, Z. Phys. B **54**, 357 (1984).
[29]H. Risken, *The Fokker-Planck Equation* (Springer, New York, 1984), Chap. 11.
[30]R. Graham and T. Tél, Phys. Rev. A **33**, 1322 (1986).
[31]R. Cristiano and P. Silvestrini, J. Appl. Phys. **59**, 1401 (1986).
[32]R. Graham states in a private communication that the values for the quasipotential given in Fig. 7 of Ref. 30 are incorrectly scaled and the quasipotential at the limit cycle is -14.7 rather than the given value of -8.8.

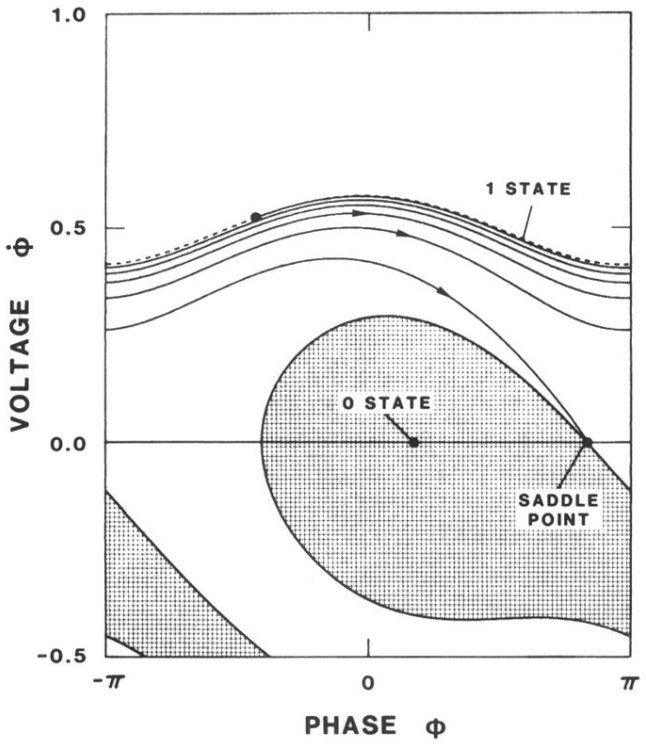

FIG. 11. State-space diagram of an escape trajectory for the 1 state obtained by solving Eq. (24) for $\beta=25$, $i_0=0.5$, and $t_e=100$. The escape trajectory is shown by a solid line and the periodic trajectory corresponding to the 1 state is shown by a dashed line. The crosshatched region is the basin of attraction of the 0 state.

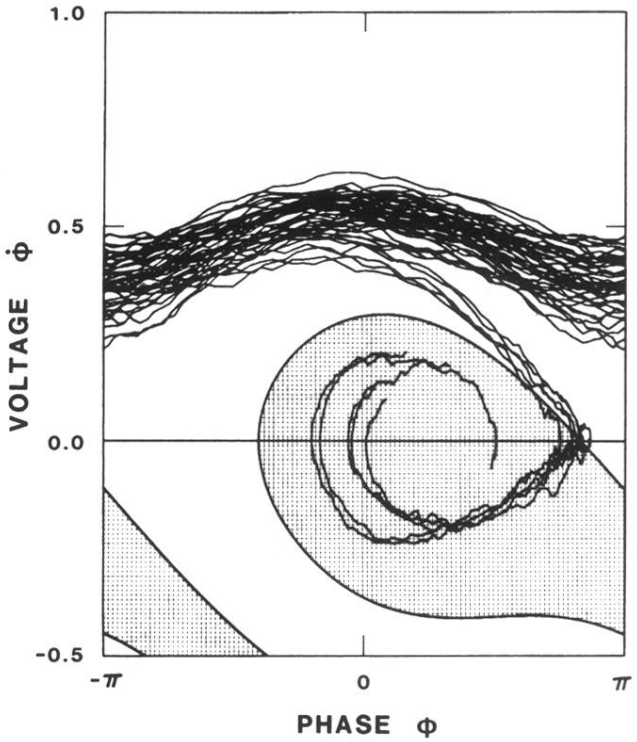

FIG. 12. State-space diagram of Monte Carlo escape trajectories for the 1 state. Five trajectories are shown for the case $\beta=25$, $i_0=0.5$, and $\Gamma=0.08$. Each trajectory is plotted over an interval of 190 time units spanning the time at which escape occurred. The crosshatched region is the basin of attraction of the 0 state.